Radiology Case Reports 15 (2020) 204–209

Available online at www.sciencedirect.com

ScienceDirect

journal homepage: www.elsevier.com/locate/radcr

Case Report

Pediatric whole body MRI detects causative ovarian teratoma in opsoclonus myoclonus syndrome

Christian Park, DO[a,*], *Imad Aljabban, MMSc*[b], *Julie C. Fanburg-Smith, MD*[c], *Christa Grant, MD*[d], *Michael Moore, MD*[e]

[a] *Department of Radiology, Penn State Health, Hershey PA 17033, USA*
[b] *Penn State College of Medicine, Hershey PA 17033, USA*
[c] *Pathology, Pediatrics, and Orthopedics, Penn State Health, Milton S. Hershey Medical Center, Hershey, PA 17033, USA*
[d] *Surgery and Pediatrics, Penn State Children's Hospital, Penn State Health, Hershey PA 17033, USA*
[e] *Radiology and Pediatrics, Penn State Health, Hershey PA 17033, USA*

ARTICLE INFO

Article history:
Received 9 September 2019
Revised 7 November 2019
Accepted 17 November 2019

Keywords:
Opsoclonus myoclonus syndrome
Ataxia
Teratoma
Pediatric
Paraneoplastic
Whole body magnetic resonance imaging (MRI)

ABSTRACT

Opsoclonus Myoclonus Syndrome (OMS, or Opsoclonus Myoclonus Ataxia) is a rare condition that presents with saccadic movements of the eyes, cerebellar ataxia, and choreiform movements of the limbs. While previous reports have described the use of ultrasound, CT, FDG-PET and traditional focused MRI for localization of OMS-associated masses, whole body MRI has not previously been reported for this purpose. Here we describe a 16-year-old patient who exhibited OMS and underwent whole body MRI to rule out the more commonly associated neuroblastoma. An ovarian mass was discovered, resected, and pathology confirmed benign teratoma - there was subsequent resolution of symptoms after complete surgical resection. Whole body MRI should be considered in pediatric cases of OMS due to the paraneoplastic nature of the disease with associated tumor, high sensitivity of disease detection, lack of ionizing radiation, excellent tissue resolution and demonstrated effectiveness in pediatric imaging.

Introduction

Opsoclonus Myoclonus Syndrome (OMS, or Opsoclonus Myoclonus Ataxia) is a rare condition that presents with saccadic movements of the eyes, cerebellar ataxia, and choreiform movements of the limbs [1]. Patients may also have neurologic symptoms such as tremor, dysarthria, and high antibody titers [2]. Most commonly observed in the pediatric population, this syndrome and constellation of symptoms is often associated with neuroblastoma [3]. In rare cases, other lesions such as a benign teratoma can lead to OMS, which can be reversed with tumor removal [1,4,5]. Therefore, prompt detection and treatment of these tumors is paramount to optimal outcome.

Previous cases have prescribed the use of ultrasound, CT, FDG-PET, and traditional focused MRI to scan for localization of OMS-associated masses. Whole body MRI has not previously been reported for this purpose. Whole body MRI has

* Corresponding author.
E-mail address: Cpark@pennstatehealth.psu.edu (C. Park).
https://doi.org/10.1016/j.radcr.2019.11.010

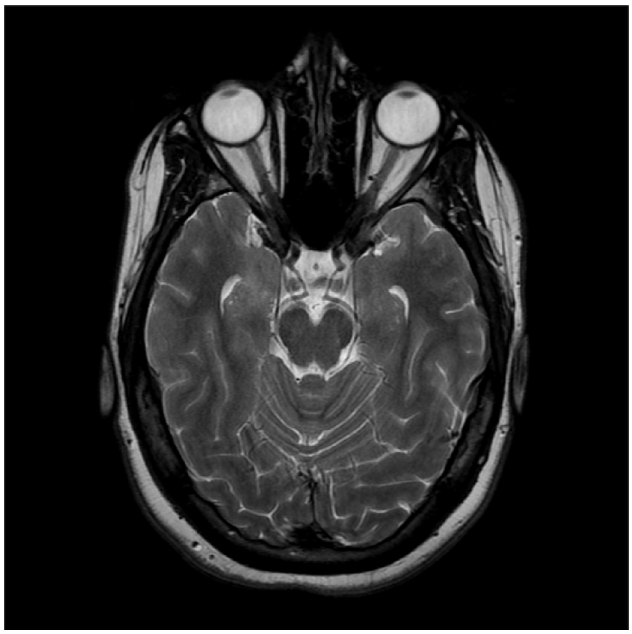

Fig. 1 – Normal brain MRI – initial imaging evaluation included brain MRI – MRA imaging at time of presentation. Axial T2 weight images demonstrated no abnormality.

been increasingly used in pediatric oncologic conditions due to technological advances, high soft tissue resolution as well as reduced acquisition times and elimination of ionizing radiation exposure [6,7]. This case report describes a pediatric patient with clinical signs of OMS where whole-body MRI was critical in making the diagnosis.

Case report

The patient is a 16-year-old female with a nonsignificant past medical history who presented with 1 week of persistent headache, expressive aphasia, ataxia, and nausea. Physical examination was significant for vertical nystagmus and dysmetria. Initial laboratory studies including a basic metabolic panel, complete blood count, and urinalysis were unremarkable. MRI and MRA of the brain and neck was normal (Fig. 1). The patient was admitted to the hospital for further evaluation.

Cerebral spinal fluid analysis was significant for moderately elevated nucleated cells, but negative for red blood cells, lymphocytes, glucose, protein, or organisms, making an infectious etiology unlikely. Paraneoplastic autoantibody evaluation of the cerebral spinal fluid for AGNA-1, amphiphysin, ANNA-1, ANNA-2, ANNA-3, CRMP-5-IgG, PCA-1, PCA-2, and PCA-Tr were negative. Ophthalmic evaluation revealed healthy optic nerves with no edema. In addition, serum aquaporin 4 receptor antibodies were negative suggesting against neuromyelitis optica or multiple sclerosis. To rule out juvenile myoclonic epilepsy, an EEG was completed and did not show epileptiform discharges.

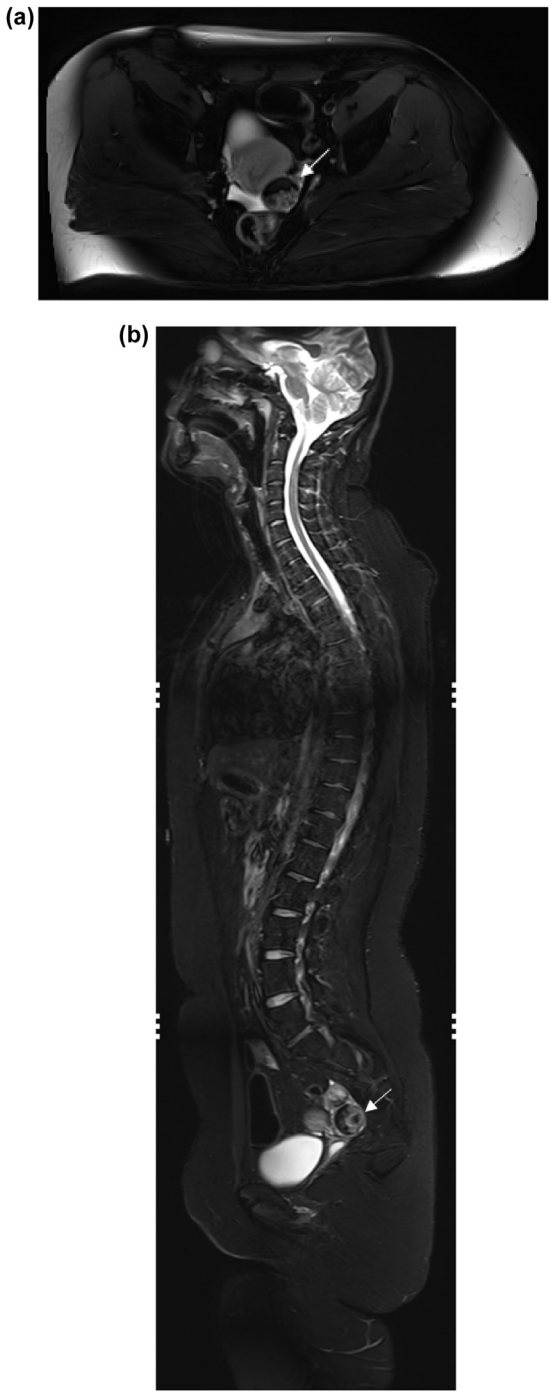

Fig. 2 – (a) Axial T2 with fat saturation image demonstrates rounded lesions with low signal intensity (suspected fat) and dependent material of mixed heterogeneity adjacent to the left ovary (arrow). (b) Sagittal STIR whole body. Rounded lesions adjacent to left ovary with heterogeneous debris in the posterior inferior portion with adjacent low signal intensity (suspected fat).

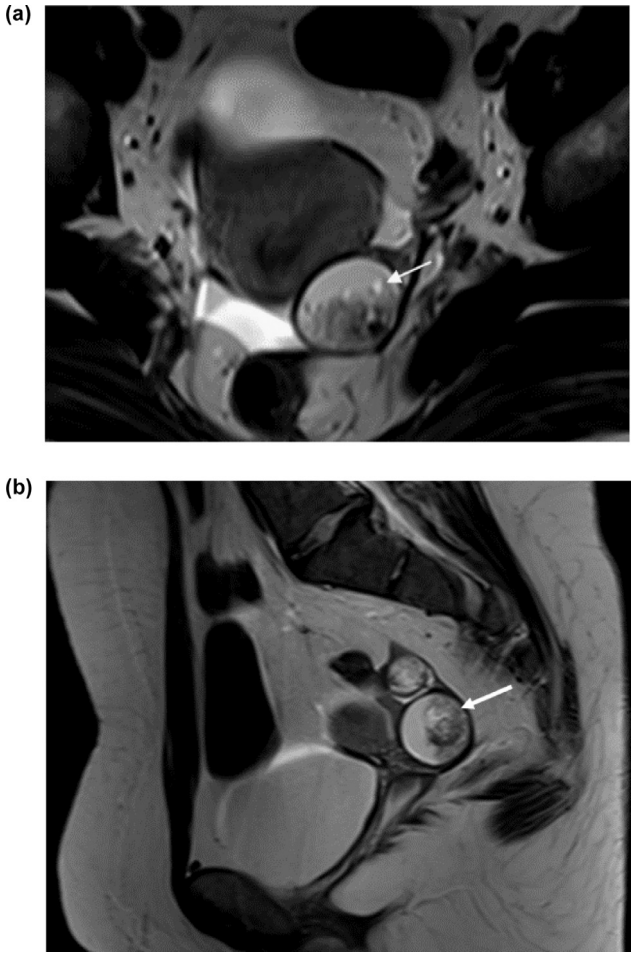

Fig. 3 – Axial (a) and sagittal (b) T2 (without fat saturation) with smaller field of view confirms the presence of fat within this lesion, heterogeneous debris of medium signal intensity (arrow), also punctate voxels of low signal intensity which represents a calcification.

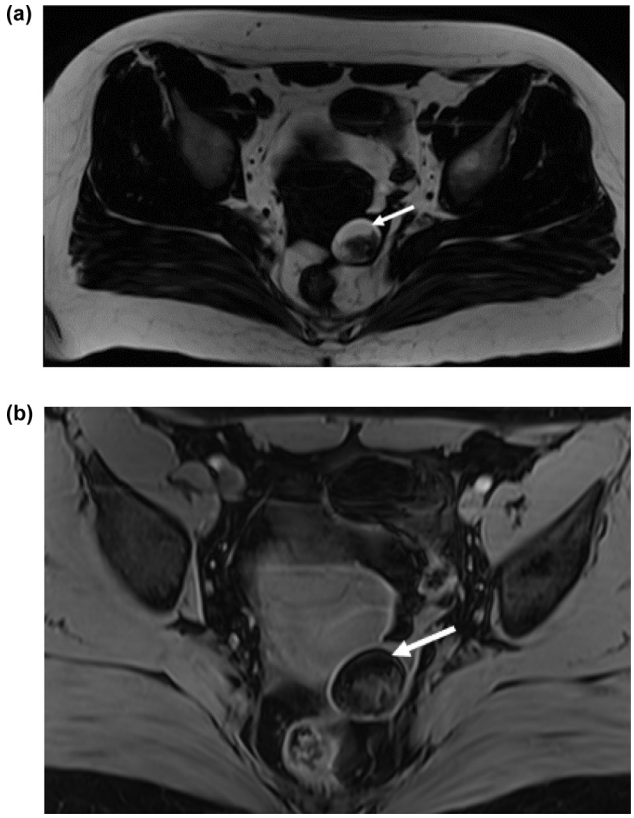

Fig. 4 – Dixon T1 sequence fat specific (a) and water specific (b) further confirmed the presence of macroscopic fat within the left ovarian teratoma.

Finally, full body MRI was performed to evaluate for neuroblastoma, a common cause of opsoclonus-myoclonus-ataxia (OMA). The whole body MRI was performed on a 3T magnet system (Siemens Skyra, Erlangen, Germany) with the patient "mummified" by overlying phased array body flex coils (18 channel) to supplement the head (20 channel) and imbedded spine coil. As part of our children's hospital standard whole body protocol coronal STIR (5 mm slices @20% gap) from the apex of the head through proximal femur; axial T2 HASTE (6 mm slices @20% gap) of the entire chest abdomen and pelvis); coronal STIR of entire spine (6 mm slices @20% gap). This patient took 42 minutes to acquire these core images. The standard protocol was modified for the clinical question and coronal STIR of lower extremities were therefore excluded in this case. The images were then checked by a Pediatric Radiologist. To further characterize the pelvic teratoma additional supplemental sequences of the pelvis were added on including axial and sagittal T2 TSE, axial T1 Dixon, 3D volumetric T1 spoiled gradient echo before and after gadolinium administration (Volumetric Interpolated Breathhold Examination), and diffusion weighted imaging. Gadobutrol 0.1 mL/kg was administered (Gadavist; Bayer AG, Leverkusen, Germany). These additional sequences added another 23 minutes to acquisition time. The study was performed without sedation.

A left ovarian teratoma measuring 3.5 × 3.3 cm was identified (Figs. 2–5). The patient was evaluated for removal of the teratoma, as it was believed to be the cause of her OMA syndrome.

A diagnostic laparoscopy was performed. There was no peritoneal studding or liver nodules. The right ovary, uterus, and both fallopian tubes appeared normal. The mass on the left ovary was identified and the nodule was dissected using electrocautery. A laparoscopic ovarian sparing partial oophorectomy was performed. The ovarian soft tissue measured at 2.8 × 2.5 × 1.8 cm weighing 6 g and had a gray-white glistening exterior. The mass was sectioned revealing a cystic cavity filled with gray-white mucoid material and hair. The final pathologic diagnosis was mature cystic teratoma. Postoperatively the patient had slight improvement of her symptoms but remained significantly neurologically impaired. There was partial improvement of her constant, spontaneous, arrhythmic multidirectional saccades. She was still experiencing frequent dysmetria and intermittent myoclonic jerks. On post-op day 5 the patient was discharged to rehabilitation therapy. No imaging was obtained in the post-operative period.

Four weeks after initial imaging the patient presented with worsening symptoms. Repeat MRI (Fig. 6) showed a mass on

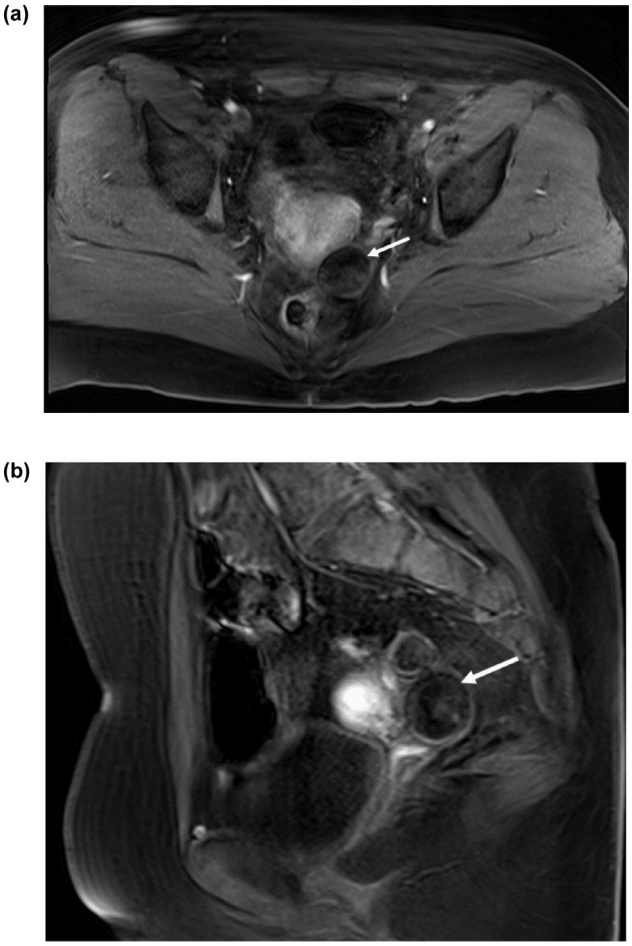

Fig. 5 – Axial (a) and sagittal (b) 3d volumetric gradient echo sequence post gadolinium demonstrates no signal enhancement VIBE = 3d volumetric interpolated breath-hold sequence [8].

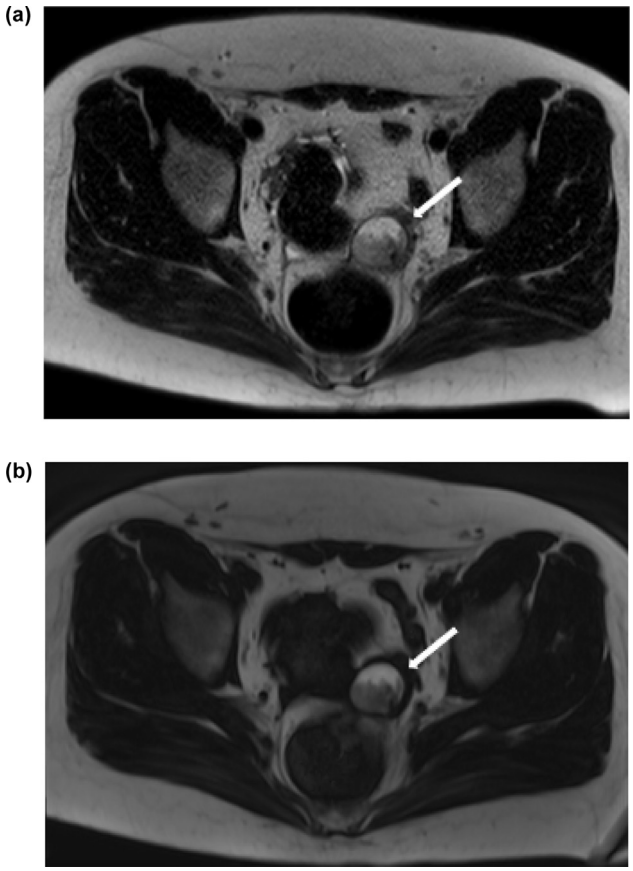

Fig. 6 – MRI at time of representation again showed a cystic mass on the left ovary with characteristics similar to the prior mass including fat. Axial T2 Haste (a) and axial Dixon fat selective (b) sequences at representation of symptoms. As both preceding operative notes and pathology reports verifying the previous resection, this was most consistent with recurrence.

the left ovary measuring 3.4 cm. As the radiologic characteristics were similar to the prior mass with both preceding operative notes and pathology reports verifying the previous resection, this was most consistent with recurrence. Lumbar puncture again resulted in all normal values. The patient was started on a course of IV methylprednisone 1 gram daily for 5 days and was taken back to the operating room. Laparoscopy again revealed a normal appearing right ovary, but the left ovary was enlarged. A distinct plane could not be visualized between the mass and normal ovarian tissue. Due to this, and given the short interval to recurrence, the decision was made to perform oophorectomy rather than a second ovary sparing procedure. Sectioning of the ovary, during gross pathology, revealed a multilocular surface with smooth walled cysts containing tan-white, grumous material admixed with white hair. Histopathology (Fig 7) revealed residual solid and cystic mature teratoma of predominantly highly differentiated, adult-type, tissue, displayed in a variably organized manner. All 3 components of ectoderm, including skin, sebaceous gland, and brain; mesoderm, including hypocellular fibrous stroma admixed with other mesenchymal elements; and endoderm, composed of enteric and respiratory tissue, were observed. There was no high grade malignant epithelial, mesenchymal or germ cell differentiation.

The patient recovered well and was discharged to rehabilitation on postoperative day 5. At discharge, her opsoclonus-myoclonus was less pronounced and dysarthria had improved, but she continued to experience dysmetria. She was seen in pediatric surgery clinic at week 18; despite some deconditioning, her symptoms had resolved.

Discussion

There is a paucity of literature that describe OMS associated with ovarian teratoma in the pediatric population. [3,9] OMS has been suggested to be an autoimmune phenomenon that is found primarily in the pediatric population and has a slight female predominance. [9] There have been high titers of autoantibodies found in OMS patients, though none have been specific for the syndrome itself [1]. It is postulated that these tumors associated with OMS may be producing antibodies that are etiologic to OMS. Indeed, in a case reported by Fadare

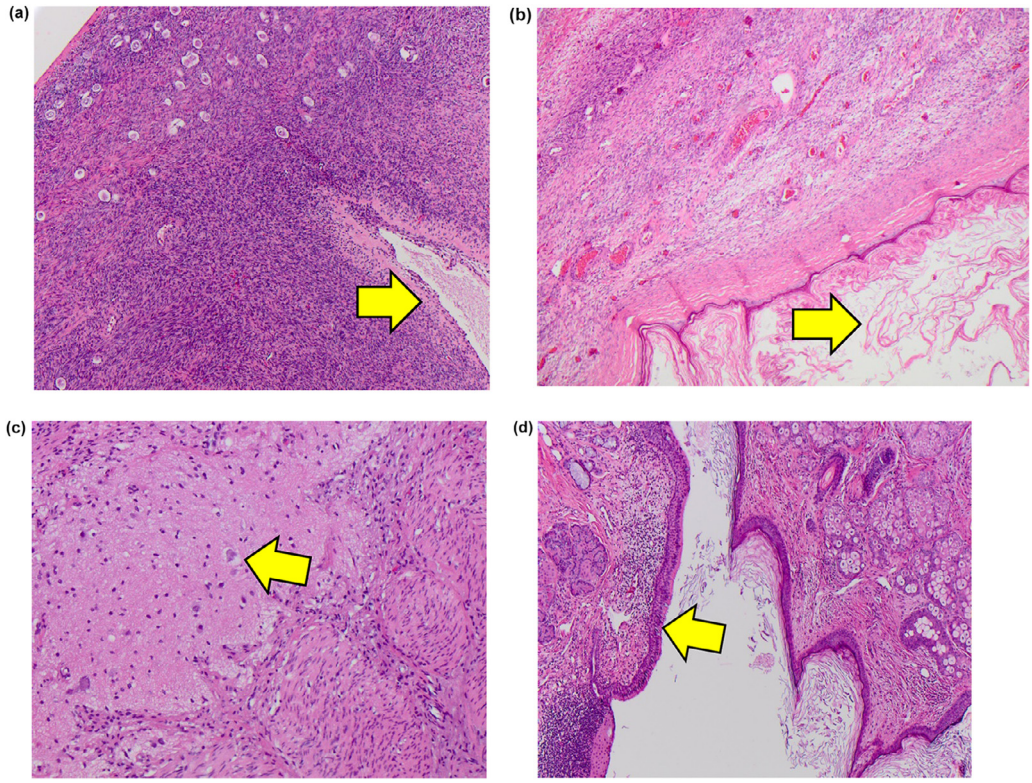

Fig. 7 – Histopathology confirms diagnosis of mature cystic teratoma with mature ectodermal, mesodermal, and endodermal tissue. (a) Histopathology (H&E, 200x) reveals normal ovarian stroma with mature cystic teratoma (arrow). (b) Histopathology (H&E, 100x) confirmed a mature teratoma with *ectoderm*, including squamous epithelium of the skin and adnexal elements with sebaceous glands and keratin (arrow) formation. (c) Histopathology (H&E, 200x) demonstrates brain (arrow) and *mesodermal* soft tissue. (d) Histopathology (H&E, 200x) reveals respiratory *endoderm* (arrow), as well as adnexal and skin squamous epithelium.

et al., a patient with OMS associated with benign ovarian teratoma was found to have an extremely high titer of an IgG autoantibody ANNA-2 that is associated with neurologic disorders [2]. Resolution of OMS after tumor resection provides further evidence that the causal agent of these neurologic constellation of symptoms is the teratoma [2].

Surgical resection enters the treatment algorithm for OMS thought to be caused by solid tumors. While there have been many case reports of OMS as a paraneoplastic syndrome associated with many tumors such as breast cancer, melanoma, and nonsmall cell lung cancer, neuroblastoma is the most common cause in pediatric patients. In adolescent and adult females, ovarian teratomas have also been reported with some frequency [10,11]. In our patient, laparoscopic resection was accomplished promptly, with recovery not otherwise affecting her clinical picture. To our knowledge, this is the only report of a short term recurrence of a benign teratoma following complete ovary sparing resection. Despite a small risk of metachronous tumors or recurrence following resection, fertility preservation facilitated by sparing healthy ovarian tissue remains an important tenet of surgery when resecting benign tumors in pediatric patients [12,13].

As tumor-associated OMS is known to have a severe clinical course, expeditious diagnosis by radiological imaging and pathologic concurrence provides the best outcome for neurologic recovery. Prompt radiologic detection and surgical resection of these lesions is paramount to optimal prognosis [5]. A number of imaging modalities have been described in the literature, however, each has its own distinct disadvantages [14]. CT and PET, while allowing adequate detection of some lesions, have significantly less soft tissue contrast resolution and exposes the patient to substantial amounts of ionizing radiation, a concern particularly in the pediatric population. Ultrasound can also be utilized to eliminate radiation; however, it is highly operator dependent and does not allow for whole body analysis.

Previously, whole body MRI for pediatric oncologic disease detection was not feasible due to the long acquisition times leading to breathing artifacts, patient noncompliance and incomplete studies [6]. Advancements in MR imaging technology such as moving table platforms, multi-channel/element surface coils, parallel imaging and novel sequences have reduced acquisition times and improved study quality significantly, leading to increased clinical use [7]. The applications of this imaging modality are broad, ranging from malignancy screening (ie, Li-Fraumeni syndrome, neurofibromatosis) to vascular indications (ie, Takayasu arteritis) [6]. Another well-established indication is evaluation of the osseous structures for chronic recurrent multifocal osteomyelitis. Specific whole body MRI protocols are variable depending on the underlying

indication and institution. At a minimum, a coronal STIR is performed at sequential gantry positions and reviewed individually prior to composition. Most institutions also utilize axial STIR or HASTE sequences as well. Further discussion is beyond the scope of this report; readers are referred to recent literature for more comprehensive description of whole body MRI in children [15]. At our institution we routinely utilize coronal STIR of the entire body, sagittal STIR of the spine, and axial HASTE with fat saturation of the chest, abdomen, and pelvis. Our hospital's most common indications in routine clinical practice include whole body tumor screening as well as evaluation for lesions in chronic recurrent multifocal osteomyelitis and osteonecrosis.

In our patient presenting with OMS, the concern was for an underlying neuroblastoma, a tumor that is associated with it in 50% of cases. As the main concern was detection of the lesion without exposure to ionizing radiation and superior soft tissue resolution of the sympathetic chain and adrenal glands, a whole body MRI was performed using a 3T magnet with STIR focused sequence. This sequence not only allows for excellent signal to background contrast ratio, but is also preferred to other fat suppression sequences for imaging across large body parts [6,10,16].

Though there is a clear temporal relationship between the surgical teratoma resection and subsequent resolution of symptoms, we cannot fully elucidate the entire underlying mechanism although this is likely a paraneoplastic phenomenon. Additionally, as anticipated with case reports, the rarity of the condition makes it difficult for generalization. Regardless, it is the role of case reports to describe infrequent conditions to help guide clinicians in their own patient with similar uncommon clinical circumstances.

Our patient's rapid recovery after tumor resection reveals the critical nature of prompt detection and treatment of OMS associated lesions. Whole Body MRI should be considered in pediatric cases of OMS due to the paraneoplastic nature of the disease with associated tumor, high sensitivity of disease detection, lack of ionizing radiation, excellent tissue resolution and demonstrated effectiveness in pediatric imaging.

REFERENCES

[1] Na CJ, Jeong YJ, Lim ST, Sohn M-H, Jeong H-J. 18F-FDG PET/CT brain imaging on a patient with paraneoplastic opsoclonus-myoclonus syndrome arising out of a mature cystic teratoma. Clin Nucl Med 2016;41(2):e104–6. doi:10.1097/RLU.0000000000001046.

[2] Fadare O, Hart HJ. Anti-ri antibodies associated with short-term memory deficits and a mature cystic teratoma of the ovary. Int Semin Surg Oncol 2004;1(1):11. doi:10.1186/1477-7800-1-11.

[3] Rudnick E, Khakoo Y, Antunes NL, Seeger RC, Brodeur GM, Shimada H, et al. Opsoclonus-myoclonus-ataxia syndrome in neuroblastoma: clinical outcome and antineuronal antibodies-a report from the Children's Cancer Group Study. Med Pediatr Oncol 2001;36(6):612–22. doi:10.1002/mpo.1138.

[4] Urriola NX, Helou J, Maamary J, Pogson J, Lee F, Parratt K, et al. NMDA receptor antibody in teratoma-related opsoclonus-myoclonus syndrome. J Clin Neurosci 2018;58:203–4. doi:10.1016/j.jocn.2018.10.011.

[5] Lou E, Hensley ML, Lassman AB, Aghajanian C. Paraneoplastic opsoclonus-myoclonus syndrome secondary to immature ovarian teratoma. Gynecol Oncol 2010;117(2):382–4. doi:10.1016/j.ygyno.2010.01.017.

[6] Eutsler EP, Khanna G. Whole-body magnetic resonance imaging in children: technique and clinical applications. Pediatr Radiol 2016;46(6):858–72. doi:10.1007/s00247-016-3586-y.

[7] Schooler GR, Davis JT, Daldrup-Link HE, Frush DP. Current utilization and procedural practices in pediatric whole-body MRI. Pediatr Radiol 2018;48(8):1101–7. doi:10.1007/s00247-018-4145-5.

[8] Inaoka T, Sugimori H, Sasaki Y, et al. VIBE MRI for evaluating the normal and abnormal gastrointestinal tract in fetuses. AJR Am J Roentgenol 2007;189(6):W303–8. doi:10.2214/AJR.07.2063.

[9] Nussinovitch U, Shoenfeld Y. The role of gender and organ specific autoimmunity. Autoimmun Rev 2012;11(6-7):A377–85. doi:10.1016/j.autrev.2011.11.001.

[10] Kanno K, Kin S, Hirose M, Suzuki S, Watanabe T, Fujimori K. Opsoclonus-ataxia syndrome associated with ovarian mature teratoma. J Obstet Gynaecol Res 2015;41(7):1149–53. doi:10.1111/jog.12675.

[11] Fitzpatrick AS, Gray OM, McConville J, McDonnell GV. Opsoclonus-myoclonus syndrome associated with benign ovarian teratoma. Neurology 2008;70(15):1292–3. doi:10.1212/01.wnl.0000308947.70045.7a.

[12] Rogers EM, Allen L, Kives S. The recurrence rate of ovarian dermoid cysts in pediatric and adolescent girls. J Pediatr Adolesc Gynecol 2014;27(4):222–6. doi:10.1016/j.jpag.2013.11.006.

[13] Abbas PI, Dietrich JE, Francis JA, Brandt ML, Cass DL, Lopez ME. Ovarian-sparing surgery in pediatric benign ovarian tumors. J Pediatr Adolesc Gynecol 2016;29(5):506–10. doi:10.1016/j.jpag.2016.03.009.

[14] Prabhu SP. Neuroimaging in pediatric opsoclonus-myoclonus syndrome: beyond the search for neuroblastomas. Dev Med Child Neurol 2015;57(3):212–13. doi:10.1111/dmcn.12598.

[15] Gottumukkala RV, Gee MS, Hampilos PJ, Greer M-LC. Current and emerging roles of whole-body MRI in evaluation of pediatric cancer patients. Radiographics 2019;39(2):516–34. doi:10.1148/rg.2019180130.

[16] Krinsky G, Rofsky NM, Weinreb JC. Nonspecificity of short inversion time inversion recovery (STIR) as a technique of fat suppression: pitfalls in image interpretation. AJR Am J Roentgenol 1996;166(3):523–6. doi:10.2214/ajr.166.3.8623620.